

Mesoporous Nitrogen-Doped Carbon for the Electrocatalytic Synthesis of Hydrogen Peroxide

Tim-Patrick Fellingner,^{*,†} Frédéric Hasché,[‡] Peter Strasser,[‡] and Markus Antonietti[†]

[†]Department of Colloids, Max Planck Institute of Colloids and Interfaces, Wissenschaftspark Golm, D-14424 Potsdam, Germany

[‡]Department of Chemistry, Technische Universität Berlin, Straße des 17 Juni 124, D-10623 Berlin, Germany

S Supporting Information

ABSTRACT: Mesoporous nitrogen-doped carbon derived from the ionic liquid *N*-butyl-3-methylpyridinium dicyanamide is a highly active, cheap, and selective metal-free catalyst for the electrochemical synthesis of hydrogen peroxide that has the potential for use in a safe, sustainable, and cheap flow-reactor-based method for H₂O₂ production.

Hydrogen peroxide is one of the 100 most important chemicals in the world.¹ The most elegant and efficient reaction pathway would be the direct conversion of elemental hydrogen and oxygen.² However, such a process creates the danger of explosion. Electrochemical flow reactors, such as the polymer electrolyte membrane fuel cell (PEMFC), represent an attractive alternative by separating oxygen reduction and hydrogen oxidation under cogeneration of energy.^{3,4} Therefore continuous research on improving the electrochemical synthesis of hydrogen peroxide is carried out,^{5–12} but electrocatalysts still suffer from high costs, limited selectivity or low activity. We herein show ionic liquid-derived mesoporous nitrogen-doped carbon to be a highly active, cheap, and selective metal-free catalyst for the electrochemical synthesis of hydrogen peroxide with the potential to establish a safe, sustainable, and cheap flow-reactor-based production method.

With the synthesis of novel mesoporous metal-free catalysts for the oxygen reduction reaction (ORR) in hydrogen fuel cells with activities in basic media comparable to those of commercial platinum catalysts, we and others could recently endorse the thesis of highly ORR-active nitrogen-doped carbon.^{13,14} However, our nitrogen-doped carbon catalysts also possess considerably high catalytic activity in the acidic media of polymer electrolyte membrane fuel cells (PEMFCs).¹³

Mechanistic analysis of the electrochemical process showed that the number of transferred electrons was not always four, as theoretically expected for the complete reduction of O₂ to H₂O; in some cases, lower, uneven values were calculated. These mixed processes indicate the presence of varying reactivity for different C–N substructures (such as pyridinic, pyrrolic, or quaternary). This in turn presented the hope of finding a selective and efficient electrocatalyst for a pure two-electron process from oxygen toward H₂O₂ on the basis of nitrogen-containing conductive carbons. According to a principal method that has already been described in detail elsewhere,^{15–17} the ionic liquid *N*-butyl-3-methylpyridinium dicyanamide (BMP-dca) was employed as direct precursor for

the synthesis of nitrogen-doped carbon (BMP-800). A simple hard-templating (nanocasting) strategy using commercial silica nanoparticles (Ludox HS40) gave the mesoporous (pore size 2–50 nm) nitrogen-doped carbon (meso-BMP-800) catalyst.

High-resolution transmission electron microscopy (HRTEM) revealed the low long-range-ordered characteristic structure of BMP-800 (Figure 1A). Graphite-like sheets are

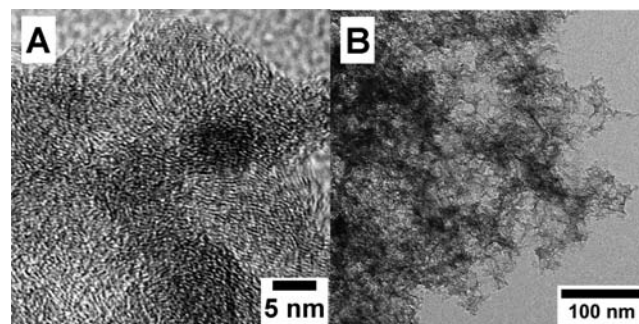


Figure 1. TEM micrographs of (A) BMP-800 and (B) meso-BMP-800.

present as a result of the high amount of structurally integrated nitrogen (16.2 wt %). Despite the apparently disordered structure, doping leads to high electrical conductivity and stability and therefore to highly desired properties for electrocatalysis.¹⁵ The successful introduction of mesopores in meso-BMP-800 was initially visualized via TEM imaging, demonstrating the structure of replicated inorganic nanoparticles after carbonization of the hybrid silica/ionic liquid material and subsequent removal of the template (Figure 1B).

Nitrogen sorption measurements on meso-BMP-800 confirmed the high specific surface area of ~320 m² g⁻¹, which at the same time is the catalytically active surface. A type-IV isotherm with a hysteresis at high relative pressure ($p/p_0 > 0.7$) was observed, which is indicative of mesoporous materials (Figure 1S in the Supporting Information). Pore analysis via a nonlocal density functional theory (NLDFT) model for slit- and cylindrical-shaped pores revealed a mean pore diameter of 13.2 nm, corresponding well with the pore diameters measured from the TEM images and the reported diameter of 13.2 nm for the commercial silica particles.¹⁸ Wide-angle X-ray scattering (WAXS) (Figure 2S) showed characteristic interlayer

Received: January 3, 2012

Published: February 16, 2012

(002) and intralayer (101) diffraction peaks at $2\theta = 26.14^\circ$ and 42.98° , respectively, and confirmed the removal of silica template. The mean interlayer distance of 340.6 pm is relatively long in comparison with graphite (335.4 pm) and results from the bent carbon structuring as observed by HRTEM. As evaluated by X-ray photoelectron spectroscopy (XPS) and elemental analysis (EA), the nitrogen content of 14.2 wt % (XPS)/17.17 wt % (EA) was very high. The variation of the values can be explained by the surface specificity of XPS measurements. In the range of its sensitivity, XPS measurements at the same time confirmed the nonmetal character of the catalyst (Fe content 0% and no indication of other metals; Figure 3S).

For the electrochemical tests representing the cathode half-cell performance of the meso-BMP-800 catalyst in a common flow cell reactor, the rotating-disk electrode (RDE) technique was used. A catalyst suspension was prepared with pure water, 2-propanol, and Nafion as a binder. An aliquot of the suspension was deposited and dried on a well-polished glassy carbon electrode and employed in RDE experiments in 0.1 M HClO₄. The acidic conditions mimicked fuel cell conditions, where protons are supplied from the anodic hydrogen oxidation reaction by diffusion through the polymer electrolyte membrane. The polarization curves at various rotation rates (representing different oxygen supplies) and the cyclic voltammogram (CV) in deaerated 0.1 M HClO₄ were recorded. The CV profile for meso-BMP-800 (Figure 2 inset)

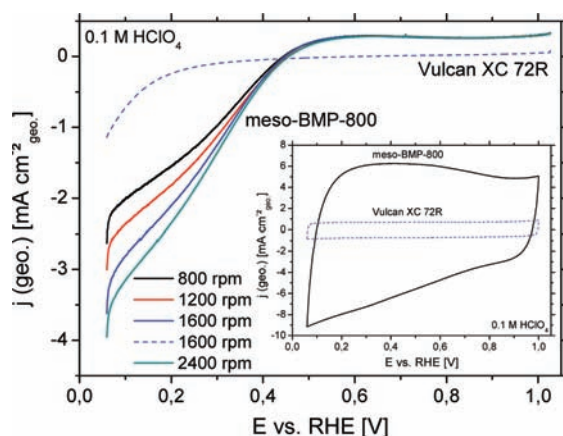


Figure 2. Electrochemical characterization of the meso-BMP-800 catalyst compared with the commercial Vulcan XC 72R carbon: Polarization curves at various rotation rates in oxygen-saturated 0.1 M HClO₄ and (inset) cyclic voltammogram measured without rotation in deaerated 0.1 M HClO₄.

shows a nearly rectangular shape indicating the high conductivity of carbon and an increased capacitive current relative to the commercial carbon.

Remarkably, in the presence of oxygen, the catalyst showed high current density polarization curves and a strongly improved overpotential (i.e., the electrochemical activation energy) relative to commercial carbon (Vulcan XC 72R, specific surface area $\sim 210 \text{ m}^2 \text{ g}^{-1}$). Therefore, meso-BMP-800 exhibits high catalytic activity for the ORR, even in an acidic medium. To investigate the kinetic reaction mechanism of the electron process, we used the Koutecky–Levich (KL) plot (Figure 3), which was obtained from the polarization curves at various rotation speeds. In the KL model, the current density

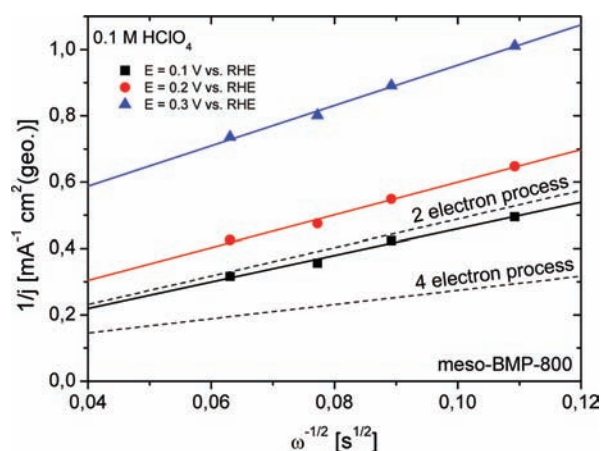


Figure 3. Koutecky–Levich plot for the determination of the number of electrons transferred during the reaction. The B factor was calculated from the slope of the KL plot using eq 1.

(j) consists of a kinetic part (j_{kin}) and a diffusion part (j_{diff}), as shown in eq 1:

$$\frac{1}{j} = \frac{1}{j_{\text{kin}}} + \frac{1}{j_{\text{diff}}} = \frac{1}{j_{\text{kin}}} + \frac{1}{B \cdot \sqrt{\omega}} \quad (1)$$

in which the B factor is given by

$$B = 0.62 \cdot z \cdot F \cdot D_{\text{O}_2}^{2/3} \cdot \nu^{-1/6} \cdot c_{\text{O}_2}$$

where z is the number of electrons transferred during the reaction, D_{O_2} and c_{O_2} are the diffusivity and solubility of oxygen, respectively, F is the Faraday constant, and ν is the kinematic viscosity of the electrolyte. For a four-electron process, $B(4e^-) = 0.47 \text{ mA cm}^{-2} \text{ s}^{1/2}$, and for a two-electron process, $B(2e^-) = 0.23 \text{ mA cm}^{-2} \text{ s}^{1/2}$.^{19,20} Figure 3 clearly shows that the experimentally determined slopes at different potentials are in good agreement with the theoretically calculated slope for a two-electron process, indicating the selective formation of hydrogen peroxide. From the experimental data, B was calculated as $0.21 \pm 0.04 \text{ mA cm}^{-2} \text{ s}^{1/2}$. The number of transferred electrons therefore calculates to 2 with a deviation of less than 9%, indicating a pure two-electron mechanism. Thus, the electrochemical analysis confirmed the high catalytic activity of meso-BMP-800 for the selective reduction of oxygen to hydrogen peroxide even in an acidic medium, following the reaction equation $\text{O}_2 + 2\text{H}^+ + 2e^- \rightarrow \text{H}_2\text{O}_2$.

To further illustrate the catalyst's selectivity, we compared the CVs obtained in deoxygenated electrolyte before and after the addition of H₂O₂. In both cases, no reduction peak or Faradaic current was observed, while subsequent oxygen purging led to strong reduction currents (Figure 4S).

High-resolution XPS spectra of the nitrogen N 1s signal revealed the presence of pyridinic (43.8% at 398.4 eV), pyrrolic (17.8% at 399.8 eV), quaternary (33% at 401.0 eV), and a few *N*-oxidic (6.1% at 402.9 eV) nitrogens. The only difference in comparison with the previously described BMP-dca-derived carbons at 1000 °C was the increased relative appearance of pyridinic and quaternary nitrogens.¹⁵ Theoretical considerations on quaternary nitrogen in graphite layers by Sidik et al.²¹ suggested a feasible mechanism for the activation of adsorbed oxygen and indicated a two-electron mechanism due to the strong binding of nitrogen-bound “radical” carbon atoms. Using simulations, Okamoto²² deduced an enforced adsorption of

oxygen molecules on C=C double bonds as the number of neighboring nitrogen atoms was increased. They could actually explain two- as well as four-electron processes within their system.

Furthermore, the electrochemical H₂O₂ production and accumulation was tested and verified for the purpose of a more intuitive demonstration employing photometrical methods. For that, the H₂O₂ was produced using the simple three-electrode catalyst test setup with a rotation speed for the working electrode of 1600 rpm in an acidic medium and a catalyst loading of $\sim 325 \mu\text{g cm}_{\text{geo}}^{-2}$. The electrolyte (0.1 M HClO₄) was continuously gas-flushed (226 mL min^{-1}) with O₂, and the working voltage was set constant at $E = 0.1 \text{ V vs RHE}$ (in the high-yield range; see Figure 2). The resulting current was $-0.01 \text{ A mg}_{\text{cat}}^{-1}$. Samples were taken after certain points of time, neutralized, brought to color reaction as instructed for the commercial peroxide test, and measured photometrically (Figure 4), using the Beer–Lambert law to evaluate the effective peroxide concentrations.

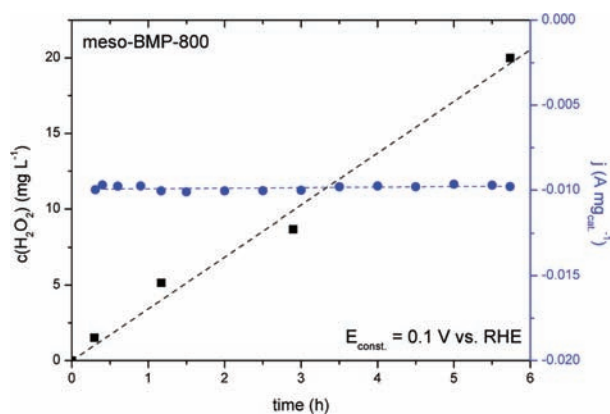


Figure 4. Photometric determination of H₂O₂ (via the Merck peroxide test) as a function of time. Current (blue ●) and concentration (black ■) behavior with time for the electrochemical H₂O₂ production is shown.

The current and H₂O₂ formation remained stable at the constant working voltage over 5.5 h. The theoretical specific electrical energy required to produce 1 g of hydrogen peroxide is $W_{\text{spec}}^{\text{theor}} = 0.157 \text{ W h g}^{-1}$, according to the formula in the denominator of eq 2 using $z = 2$ and the molar mass (M) of H₂O₂. The actual (practical) specific energy $W_{\text{spec}}^{\text{pract}}$ expended was 0.241 W h g^{-1} , according to the numerator of eq 2 using the mean current I (0.63 mA), the reaction time t (5.74 h), the working voltage E (0.1 V vs RHE), and the resulting mass of H₂O₂ (1.5 mg) calculated from concentration c_m and the electrolyte volume V . Hence, the faradaic efficiency ε_F (eq 2) is 65.15%, which can be explained by the concurrent disproportionation of the peroxide in the acidic medium.

$$\varepsilon_F = \frac{W_{\text{spec}}^{\text{pract}}}{W_{\text{spec}}^{\text{theor}}} = \frac{I \cdot t \cdot E}{z \cdot F \cdot E} \cdot \frac{c_m \cdot V}{M} \quad (2)$$

The use of the as-presented cheap, nonmetal electrocatalyst in an adequate production setup, such as a fuel-cell-type flow reactor, is especially (but not exclusively) attractive in terms of flexibility. Hydrogen peroxide could be synthesized in small amounts directly at the place of need (e.g., in a washing

machine) and at the right point in time. Additionally, the method is very inexpensive (regarding electricity 2.4 EUR cents $\text{kg}_{\text{H}_2\text{O}_2}^{-1}$ at 10 EUR cents kWh^{-1} industry price), while costs for the transport of liquid hazardous H₂O₂ could be avoided. As such, precise attribution of the catalytic activity to a specific binding site seems rather speculative. Besides the importance of an increased nitrogen content retaining sufficient conductivity (see ref 22), another possible factor affecting the reactivity is the degree of graphitization. Here, the polarizability of the graphitic layers should influence the adsorption properties, while the elongation of the conjugated π system could determine crucial electronic properties. As the radical character of nitrogen-bound carbon may support the two-electron process, less-conjugated π systems should be more favored for hydrogen peroxide synthesis.²¹ However, nitrogen-doped carbon materials have also received great attention as support materials for metal and metal alloy catalysts, for example, in the methanol oxidation reaction or oxygen reduction to water.^{23,24}

In conclusion, we have shown that conductive nitrogen-doped carbon is applicable as an efficient, metal-free catalyst for the selective, green, and cheap electrochemical production of hydrogen peroxide. Besides being easy and cheap, the catalyst synthesis is flexible enough to allow further optimization of the porosity and surface area.

To date, the true dependence of the structure on the reactivity remains unclear, and further investigations are needed. However, as a comparable material synthesized at higher temperatures (1000 °C) supports the four-electron process, certain assumptions can be made: (1) Consistent with simulations of Okamoto,²² an increased nitrogen content may favor the two-electron process. (2) The “radical” character of nitrogen-bound carbon, which is essential for the two-electron process,²¹ may be more pronounced for meso-BMP-800 because of the lower degree of delocalization. (3) The pyrrolic nitrogen sites within the carbon material elucidated by high-resolution XPS, which are not present at higher synthesis temperatures, might indeed contribute in an essential way to the activity of the two-electron process.

In the future, we hope to answer the question by cooperative efforts, including more detailed atomistic characterizations. Further work will also deal with analyzing the broader applicability of this sustainable class of catalysts to other elemental basic electrochemical reactions.

Methods. BMP-dca was purchased from Ionic Liquid Technologies GmbH. A 40 wt % aqueous dispersion of Ludox HS40, Nafion 117 solution (5 wt %), and NH₄HF₂ was obtained from Aldrich, and the 0.1 M KOH solution and the peroxide test kits were purchased from Merck. All chemicals were used as received without further purification. BMP-dca (2 g) was mixed with the 40 wt % Ludox dispersion (5 g), and the mixture was transferred into alumina crucibles and carbonized. The thermal treatment was conducted under a nitrogen gas flow in a VMK 80 S lab oven (Linn High Therm GmbH). After half an hour of purging, the sample was heated to 800 °C at a heating rate of 10 K min⁻¹ and an isothermal period of 1 h at 800 °C. The resulting black solid was ground and treated with 4 M NH₄HF₂ solution to remove the silica. Washing with water and subsequent drying gave a fine black powder. The electrochemical characterization was conducted using the RDE (PINE Instruments, USA) technique in a custom-made three-compartment electrochemical glass cell with a commercial potentiostat (VSP-5, BioLogic, France).^{25,26} The three-electrode setup consisted of a Pt mesh counter

electrode, a reversible hydrogen electrode (Hydroflex HREF, Gaskatel, Germany) reference electrode, and a commercial fixed glassy carbon working electrode (PINE Instruments, USA) with a diameter of 5 mm (0.196 cm²). For the preparation of the working electrode with a thin catalytic film, ~15 mg of catalyst was suspended in a mixture containing 1.99 mL of pure water, 0.5 mL of 2-propanol, and 10 μL 5 wt % Nafion solution. After sonification, 10 μL of the catalyst suspension was put onto the well-polished glassy carbon electrode and dried in air for 10 min at 60 °C. All measurements were conducted at room temperature.

■ ASSOCIATED CONTENT

📄 Supporting Information

Nitrogen sorption porosimetry data, WAXS data, XPS survey spectrum, and CVs. This material is available free of charge via the Internet at <http://pubs.acs.org>.

■ AUTHOR INFORMATION

Corresponding Author

Fellinger@mpikg.mpg.de

Notes

The authors declare no competing financial interest.

■ ACKNOWLEDGMENTS

Sören Selve (TU Berlin) and Carmen Serra (Universidad de Vigo/Spain) are kindly thanked for HRTEM and XPS measurements. The Cluster of Excellence “Unifying Concepts in Catalysis” (UniCat), the Technische Universität Berlin and the Max-Planck Society are acknowledged for financial support.

■ REFERENCES

- (1) Myers, R. L. *The 100 Most Important Chemical Compounds: A Reference Guide*; Greenwood Publishing Group: Westport, CT, 2007.
- (2) Campos-Martin, J. M.; Blanco-Brieva, G.; Fierro, J. L. G. *Angew. Chem., Int. Ed.* **2006**, *45*, 6962.
- (3) Otsuka, K.; Yamanaka, I. *Catal. Today* **1998**, *41*, 311.
- (4) Yamanaka, I.; Onisawa, T.; Hashimoto, T.; Murayama, T. *ChemSusChem* **2011**, *4*, 494.
- (5) Lunsford, J. H. *J. Catal.* **2003**, *216*, 455.
- (6) Samanta, C.; Choudhary, V. R. *Chem. Eng. J.* **2008**, *136*, 126.
- (7) Choudhary, V. R.; Jana, P. *J. Catal.* **2007**, *246*, 434.
- (8) Otsuka, K.; Yamanaka, I. *Electrochim. Acta* **1990**, *35*, 319.
- (9) Gyenge, E. L.; Oloman, C. W. *J. Appl. Electrochem.* **2001**, *31*, 233.
- (10) Lobyntseva, E.; Kallio, T.; Alexeyeva, N.; Tammeveski, K.; Kontturi, K. *Electrochim. Acta* **2007**, *52*, 7262.
- (11) Forti, J. C.; Rocha, R. S.; Lanza, M. R. V.; Bertazzoli, R. *J. Electroanal. Chem.* **2007**, *601*, 63.
- (12) Jirkovský, J. S.; Panas, I.; Ahlberg, E.; Halasa, M.; Romani, S.; Schiffrin, D. J. *J. Am. Chem. Soc.* **2011**, *133*, 19432.
- (13) Yang, W.; Fellinger, T. P.; Antonietti, M. *J. Am. Chem. Soc.* **2011**, *133*, 206.
- (14) Liu, R.; Wu, D.; Feng, X.; Müllen, K. *Angew. Chem., Int. Ed.* **2010**, *49*, 2565.
- (15) Paraknowitsch, J. P.; Zhang, J.; Su, D.; Thomas, A.; Antonietti, M. *Adv. Mater.* **2010**, *22*, 87.
- (16) Paraknowitsch, J. P.; Thomas, A.; Antonietti, M. *J. Mater. Chem.* **2010**, *20*, 6746.
- (17) Lee, J. S.; Wang, X.; Luo, H.; Baker, G. A.; Dai, S. *J. Am. Chem. Soc.* **2009**, *131*, 4596.
- (18) Singh, P. S.; Aswal, V. K. *J. Colloid Interface Sci.* **2008**, *326*, 176.
- (19) Markovic, N. M.; Gasteiger, H. A.; Grgur, B. N.; Ross, P. N. *J. Electroanal. Chem.* **1999**, *467*, 157.
- (20) Paulus, U. A.; Schmidt, T. J.; Gasteiger, H. A.; Behm, R. J. *J. Electroanal. Chem.* **2001**, *495*, 134.

(21) Sidik, R. A.; Anderson, A. B.; Subramanian, N. P.; Kumaraguru, S. P.; Popov, B. N. *J. Phys. Chem. B* **2006**, *110*, 1787.

(22) Okamoto, Y. *Appl. Surf. Sci.* **2009**, *256*, 335.

(23) Zhou, Y.; Neyerlin, K.; Olson, T. S.; Pylypenko, S.; Bult, J.; Dinh, H. N.; Gennett, T.; Shao, Z.; O’Hayre, R. *Energy Environ. Sci.* **2010**, *3*, 1437.

(24) Hasché, F.; Fellinger, T.-P.; Oezaslan, M.; Paraknowitsch, J. P.; Antonietti, M.; Strasser, P. *ChemCatChem* **2012**, DOI: 10.1002/cctc.201100408.

(25) Hasché, F.; Oezaslan, M.; Strasser, P. *Phys. Chem. Chem. Phys.* **2010**, *12*, 15251.

(26) Hasché, F.; Oezaslan, M.; Strasser, P. *ChemCatChem* **2011**, *3*, 1805.